Emergence of long-range order in $BaTiO_3$ from local symmetry-breaking distortions

M. S. Senn,[1,*] D. A. Keen,[2] T. C. A. Lucas,[3] J. A. Hriljac,[3] and A. L. Goodwin[1]

[1]*Department of Chemistry, Inorganic Chemistry Laboratory, University of Oxford, South Parks Road, Oxford OX1 3QR, United Kingdom*
[2]*ISIS, Rutherford Appleton Laboratory, Harwell Campus, Didcot OX11 0QX, United Kingdom*
[3]*School of Chemistry, University of Birmingham, Edgbaston, Birmingham, B15 2TT, United Kingdom*

(Dated: June 29, 2016)

By using a symmetry motivated basis to evaluate local distortions against pair distribution function data (PDF), we show without prior bias, that the off-centre Ti displacements in the archetypal ferroelectric $BaTiO_3$ are zone centred and rhombohedral-like across its known ferroelectric and paraelectric phases. We construct a simple Monte Carlo (MC) model which captures our main experimental findings and demonstrate how the rich crystallographic phase diagram of $BaTiO_3$ emerges from correlations of local symmetry-breaking distortions alone. Our results strongly support the order-disorder picture for these phase transitions, but can also be reconciled with the soft-mode theory of $BaTiO_3$ that is supported by some spectroscopic techniques.

PACS numbers: 77.80.-e, 77.80.Dj, 61.43.Bn,61.50.Ks

The phenomenological study of displacive phase transitions by Landau-Ginzburg theory has been exceptionally fruitful [1]. Its apparently close relationship to the theory of soft-mode phase transitions [2, 3] has meant that the expansion of the free energy of a system in terms of the correct order parameter can lead to a one-to-one correspondence with the energy of a phonon mode in the harmonic approximation. Studies of global lattice and electronic instabilities benefit from the classification of global symmetry breaking (an order parameter) in terms of irreducible representations (see [4] and references therein) of the parent symmetry space which themselves have a correspondence with the eigenvectors (harmonic phonons) of the system. Furthermore, their allowed couplings (or phonon-phonon scatterings) may be studied up to a given order by considering only those which are invariant under the parent symmetry operators [5]. This, combined with the fact that global symmetry dictates both microscopic structure and macroscopic observables in these phase transitions means that the latter, which are often more conveniently measured, may be used as the order parameter for these phase transitions. However, many macroscopic observables are a result of emergent phenomena driven by local ordering which combine in often counter-intuitive ways to produce the global symmetry of the structure. Hence the local symmetry effectively controls the physical property [6]. Here a phenomenological model based around a macroscopic (or crystallographic) parameter will not lead to a valid physical insight into the phase transition. Hence, microscopic studies of local symmetry-breaking are vital if physical understanding is to be gained.

In any crystallographic model there are many ways to locally break the average symmetry; for example, through thermal effects, distortions, or dislocations. The difficulty is to coalesce these local degrees of freedom into an understandable form within a given length-scale and to evaluate their contribution systematically against data sensitive to local correlations such as XANES, EXAFS, PDF and diffuse scattering. It is particularly desirable to compare against neutron PDF data which are sensitive to local distortions beyond a length scale of the first coordination shell. As no simple method exists for doing this, often our understanding of emergent phenomena in condensed phases is based on model building biased towards the macroscopic observables, whereas ideally these properties should emerge spontaneously from our analysis of the local structure. Here we present such a method and demonstrate its effectiveness at identifying the local order parameter in $BaTiO_3$. This provides the first unbiased local model of this system and show how the crystallographic phase transitions can emerge naturally from the correlations of the local symmetry-breaking distortions.

The ferroelectric properties of $BaTiO_3$ were first reported in the 1940s[7]. The ferroelectricity and concomitant cubic to tetragonal structural distortion [8] were initially discussed in the framework of displacive phase transitions [9]. However, the subsequent observations of orthorhombic and rhombohedral phase transitions at lower temperatures[10, 11] are inconsistent with second-order displacive phase transitions. This anomaly together with the observation of diffuse x-ray scattering in all but the low temperature rhombohedral phase [12] led to the development of the phenomenological order-disorder model [13]. This has been supported by other techniques sensitive to local order such as PDF [14] and XANES/EXAFS methods [15]. In this model, the incipient ferroelectric displacements of the Ti are taken to be rhombohedral-like, towards the faces of the TiO_6 octahedra (Fig. 2(b)), with long-range correlations in chains along ⟨100⟩, and disorder between chains giving rise to the average crystallographic symmetry. The model ex-

* mark.senn@chem.ox.ac.uk

plains the sheets of diffuse x-ray scattering observed in isostructural $KNbO_3$ [13] and removes the requirement for the phase-transitions to proceed via group-subgroup relationships. However, diffuse scattering data have been analysed in terms of soft phonon modes [16] and many spectroscopic techniques such as Raman [17, 18] and inelastic neutron [19, 20] scattering still appear to support a displacive phase transition model. Additionally, it has been shown computationally that the cubic to tetragonal phase transitions can be achieved by combining features of order-disorder and displacive type mechanisms [21]. Clearly consensus in the research community has yet to be reached.

Polycrystalline $BaTiO_3$ was prepared by conventional solid state synthesis. A 2 cm^3 sample was loaded into an 8 mm diameter cylindrical Vanadium can, and neutron powder diffraction data were collected at 500, 410, 350, 293, 250, 210, 150 and 15 K on the instrument GEM [22] at ISIS, UK. The maximum usable Q was 40 $Å^{-1}$ and counting times were 6-8 hrs. Rietveld refinements were performed in Topas. The total scattering data were corrected for background, sample container, multiple scattering, absorption and inelasticity effects using Gudrun [23] to produce the real-space pair distribution function (PDF). As we are performing our fitting procedure in PDFFit [24] we work here with $G^{\mathrm{PDF}}(r)$ which is proportional to $D(r)$ and whose relationship with other parametrisations of the PDF is given in Ref. 25.

Although visual differences are evident in the PDFs as a function of temperature (Fig. 1), modelling is required to extract the local distortions of the atoms from their high symmetry positions. Two approaches exist, one is a small box method fitting the data whilst relying on a crystallographic unit cell akin to Rietveld fitting (e.g. ref. [26]) and the other is a big box method where a large supercell is refined using reverse Monte Carlo (RMC) [27]. The problem with conventional small box PDF analysis is that the parametrization requires a priori assumption of the nature of the local distortions. Equally, in RMC refinements, where the degrees of freedom are many, there are many ways to interrogate the refined parameters and an exhaustive analysis is impractical; bias is often introduced at this stage. Recent work [28] has sought to tackle this problem by decomposing RMC configurations in terms of their zone centre irreducible representations (irreps.). However, short range correlations beyond this length scale are lost in this analysis, and the modelling / refinement stage does not make use of the inherent orthogonality of symmetry adapted displacements. In contrast, the method we use here involves expanding the degrees of freedom of the crystallographic unit cell up to a given supercell size in terms of both zone centre and zone boundary irreps. of the "parent" space group. The collection of symmetry-breaking displacements transforming as the same irrep. may be further decomposed into symmetry-adapted distortion modes (hereafter referred to simply as modes). A number of web based tools can perform this decomposition [29, 30] and this parametrization has been used successfully in Rietveld refinement to systematically test for symmetry-breaking during phase transitions. [31, 32]. We extend this further by utilizing the constraint language of PDFGui / PDFFit [24] to refine mode amplitudes directly against PDF data. Further details of the implementation are given as supplemental information (S.I.) [33] and a comprehensive description will be published elsewhere.

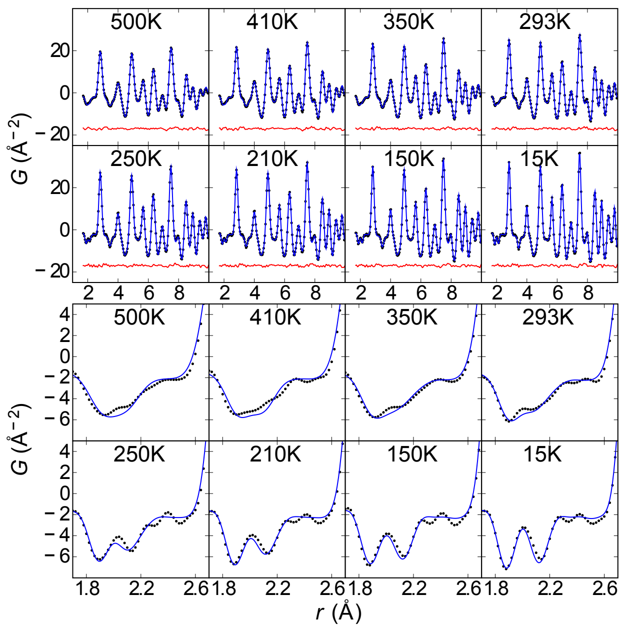

Figure 1. (color online) Fits to G(r) at the various temperatures indicated using symmetry-adapted displacements belonging to Γ_4^- irrep. only. The enlarged region around 1.8 - 2.2 Å shows the Ti-O bonds, which change most visibly as a function of temperature. The fitting procedure is described in the text.

Fig. 1 shows best fits from our data analysis procedure at each temperature. We obtain very good fits to all the PDF data, with differences between observed and calculated intensities being of the order of the Fourier ripples in the data. Of course, the parametrisation of the xyz degrees of freedom into modes does not change the overall goodness-of-fit but merely facilitates a systematic search of all parameter space. In the S.I. we also show that these fits are superior to those obtained with a big box RMC type model (noting that RMC models are also constrained to simultaneously fit the Bragg profile) and that average models from Rietveld analysis are inadequate at describing the PDF data at all but the lowest temperatures.

We performed the analysis on a $2 \times 2 \times 2$ $P1$ supercell of the $Pm\bar{3}m$ unit cell of paraelectric $BaTiO_3$, which encompasses all of the common symmetry lowering phase transitions observed in the perovskite family leading to 120 internal degrees of freedom, although our analysis can easily be extended to incorporate displacements with longer period modulations. We chose this supercell size

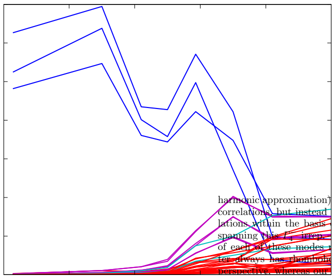

harmonic approximation)
correlations, but instead
lations within the basis
spanning this Γ_4^- irrep.
of each of these modes
ter always has rhombohe
perspective, whereas our

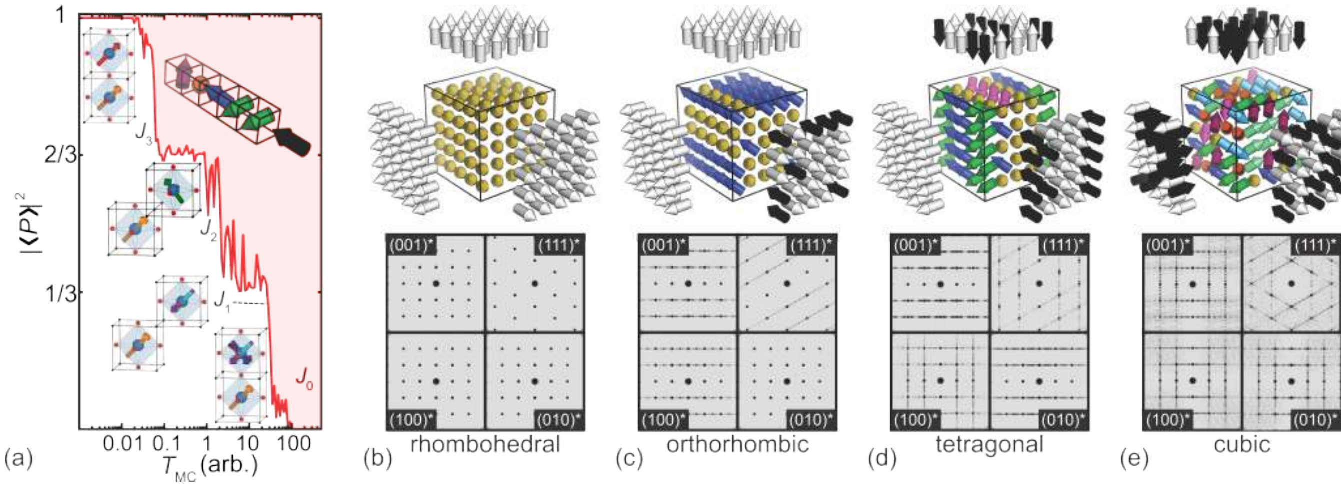

Figure 3. (color online) *a*) MC simulation reproducing the tetragonal, orthorhombic and rhombohedral phase transitions, with the square of the average polarization serving as an order parameter. Insets below the polarization line identify the relevant interactions penalized by our Hamiltonian, placed at temperatures where their energy scales become important in the simulation, and above the line, a representation of the chain like correlations present in the cubic phase (J_0, hardwired into our simulations) showing how the projection of the polarization along the direction of a chain is always preserved (black arrow). *b*)-*e*) a portion of an MC configuration for each phase, with their polar vector projections along $\langle 100\rangle$ directions, and their calculated diffuse scattering in the planes indicated. It is the inter-chain disorder between the polar vector projections (white and black arrows) which gives rise to diffuse planes of scattering in reciprocal space. In the cubic phase it is in all three $\langle 100\rangle$ directions, giving three sets of intersecting orthogonal diffuse scattering planes in reciprocal space, and each successive phase transition represent inter-chain orderings along successive $\langle 100\rangle$ directions. An enlarged version of this figure is given as part of the S.I.

$|J_3| < |J_2| < |J_1|$. $\langle i,j\rangle$ denotes a sum over nearest-neighbour sites i,j; double and triple angle brackets denote sums over second and third nearest neighbours, respectively. The three terms in this toy Hamiltonian penalise dipole misalignment in first-, second-, and third-nearest neighbour sites as shown in the inset of Fig. 3 (*a*). This Hamiltonian is the cost function for a MC simulation with a $10 \times 10 \times 10$ supercell in which all dipoles are hard-wired to have a common projection along any one chain when viewed down one of the $\langle 100\rangle$ directions (i.e. we assume a J_0 term with high energy in keeping with Ref. 13 and as illustrated in the inset of Fig. 3 (*a*)). The simulation (Fig. 3 (*a*)) shows three distinct phase transitions with discontinuities in macroscopic polarization. In Fig. 3 (*b*)-(*e*) we illustrate portions of representative configurations of the correlated disorder in the MC simulation, along with their calculated diffuse scattering. Both our calculated diffuse scattering and observed chain like configurations of off-centre Ti displacements are consistent with that published earlier [12, 13].

These MC simulations show how the observed sequence of phase transitions can arise from local correlations of nearest-neighbour type interactions alone and strongly support the order-disorder picture of $BaTiO_3$. Importantly, this order-disorder picture is not necessarily contradictory to spectroscopic results and a soft-mode picture [17–20]. When our high temperature cubic phase is viewed down any of its 4-fold axes, the correlated disorder of the Ti displacements clearly has average tetragonal symmetry. There are 6 symmetry equivalent tetragonal-like chains, in which the average Ti displacements is along one of the $\langle 100\rangle$ directions. A spontaneous symmetry-breaking event in which an inter-chain correlation length tends to infinity could be viewed as a pseudo-tetragonal soft mode phase transition. Indeed, diffuse scattering associated with the cubic to tetragonal phase transition has been shown to be equally well described by soft mode models [40, 41] which are relatively dispersionless in nature [42]. The present work hence provides a microscopic justification for why this duality in the description of the diffuse scattering exists.

Our results are the first unbiased determination of local symmetry in $BaTiO_3$ across all its known phases. They show that local displacements of the Ti atoms are zone centered and rhombohedral-like at all temperatures. The fact that a simple Hamiltonian, which considers only local interactions, can reproduce the rich phase diagram in an MC simulation gives strong support to the order-disorder picture for $BaTiO_3$ and demonstrates how global symmetry may emerge from local symmetry-breaking distortions. This fundamental insight highlights the importance of our methodology for determining local symmetry in order-disorder phase transitions and demonstrates its power when it is coupled to MC simulations. We note that recent developments in speeding up the simulation of PDF data by orders of magnitude [43] will allow the exploration of ever more complicated systems exhibiting order-disorder phase transitions, and hope that our work will stimulate research into a host of other systems exhibiting emergent phenomena.

We would like to acknowledge STFC for awarding us neutron beamtime. MSS is grateful to the Royal Commission for the Exhibition of 1851 for a fellowship, ALG for funding from the ERC (grant no. 279705) and TCAL and JAH for studentship funding from Diamond Light Source.

[1] R. A. Cowley, Adv. Phys. **29**, 1 (1980).
[2] P. Sollich, V. Heine, and M. T. Dove, J. Physics-Condensed Matter **6**, 3171 (1994).
[3] M. T. Dove, A. P. Giddy, and V. Heine, Ferroelectrics **136**, 33 (1992).
[4] H. T. Stokes, B. J. Campbell, and R. Cordes, Acta Crystallogr. Sect. A Found. Crystallogr. **69**, 388 (2013).
[5] D. M. Hatch and H. T. Stokes, J. Appl. Crystallogr. **36**, 951 (2003).
[6] D. A. Keen and A. L. Goodwin, Nature **521**, 303 (2015).
[7] A. Von Hippel, R. G. Breckenridge, F. G. Chesley, and L. Tisza, Ind. Eng. Chem. **38**, 1097 (1946).
[8] H. D. Megaw, Proc. R. Soc. A Math. Phys. Eng. Sci. **189**, 261 (1947).
[9] W. Cochran, Adv. Condens. Matter Phys. **9**, 387 (1960).
[10] H. F. Kay and P. Vousden, Philos. Mag. Ser. 7 **40**, 1019 (1949).
[11] R. G. Rhodes, Acta Crystallogr. **2**, 417 (1949).
[12] R. Comès, M. Lambert, and A. Guinier, Solid State Commun. **6**, 715 (1968).
[13] R. Comès, M. Lambert, and A. Guinier, Acta Crystallogr. Sect. A Cryst. Physics, Diffraction, Theor. Gen. Crystallogr. **26**, 244 (1970).
[14] G. H. Kwei, S. J. L. Billinge, S.-W. Cheong, and J. G. Saxton, Ferroelectrics **164**, 57 (1995).
[15] B. Ravel, E. A. Stern, R. I. Vedrinskii, and V. Kraizman, Ferroelectrics **206**, 407 (1998).
[16] M. Holma, N. N. Takesue, and H. Chen, Ferroelectrics **164**, 237 (1995).
[17] L. Rimai, J. L. Parsons, and J. T. Hickmott, Phys. Rev. **168**, 623 (1968).
[18] H. Vogt, J. Sanjurjo, and G. Rossbroich, Phys. Rev. B **26**, 5904 (1982).
[19] G. Shirane, B. Frazer, V. Minkiewicz, J. Leake, and A. Linz, Phys. Rev. Lett. **19**, 234 (1967).
[20] G. Shirane, J. D. Axe, and J. Harada, Phys. Rev. B **2**, 3651 (1970).
[21] R. Pirc and R. Blinc, Phys. Rev. B **70**, 1 (2004).
[22] P. Day, J. Enderby, W. Williams, L. Chapon, A. C. Hannon, P. Radaelli, and A. K. Soper, Neutron News **15**, 19 (2004).
[23] S. E. McLain, D. T. Bowron, A. C. Hannon, and A. K. Soper, "GUDRUN, a computer program developed for analysis of neutron diffraction data, Chilton: ISIS Facility, Rutherford Appleton Laboratory," (2012).
[24] C. L. Farrow, P. Juhas, J. W. Liu, D. Bryndin, E. S. Božin, J. Bloch, T. Proffen, and S. J. L. Billinge, J. Phys. Condens. Matter **19**, 335219 (2007).
[25] D. A. Keen, J. Appl. Crystallogr. **34**, 172 (2001).
[26] S. J. L. Billinge, Zeitschrift für Krist. **219**, 117 (2004).
[27] H. Y. Playford, L. R. Owen, I. Levin, and M. G. Tucker, Annu. Rev. Mater. Res. **44**, 429 (2014).
[28] J. R. Neilson and T. M. McQueen, J. Appl. Crystallogr. **48**, 1560 (2015).
[29] B. J. Campbell, H. T. Stokes, D. E. Tanner, and D. M. Hatch, J. Appl. Crystallogr. **39**, 607 (2006).
[30] J. M. Perez-Mato, D. Orobengoa, and M. I. Aroyo, Acta Crystallogr. Sect. A Found. Crystallogr. **66**, 558 (2010).
[31] B. J. Campbell, J. S. O. Evans, F. Perselli, and H. T. Stokes, IUCr Comput. Comm. Newsl. **8**, 81 (2007).
[32] S. Kerman, B. J. Campbell, K. K. Satyavarapu, H. T. Stokes, F. Perselli, and J. S. O. Evans, Acta Crystallogr. A. **68**, 222 (2012).
[33] See Supplemental Material [url], which includes Refs. [34-35].
[34] A. Coelho, "Topas," (2009).
[35] J. S. O. Evans, Mater. Sci. Forum **651**, 1 (2010).
[36] Q. Zhang, T. Cagin, and W. A. Goddard, Proc. Natl. Acad. Sci. U. S. A. **103**, 14695 (2006).
[37] I. Levin, V. Krayzman, and J. C. Woicik, Phys. Rev. B **89**, 024106 (2014).
[38] P. Ghosez, X. Gonze, and J. P. Michenaud, Ferroelectrics **206**, 12 (1997).
[39] R. E. Cohen, Nature **358**, 136 (1992).
[40] N. L. Matsko, E. G. Maksimov, and S. V. Lepeshkin, J. Exp. Theor. Phys. **115**, 309 (2012).
[41] A. Hüller, Solid State Commun. **7**, 589 (1969).
[42] E. Farhi, A. Tagantsev, R. Currat, B. Hehlen, E. Courtens, and L. Boatner, Eur. Phys. J. B **15**, 615 (2000).
[43] A. A. Coelho, P. A. Chater, and A. Kern, J. Appl. Crystallogr. **48**, 869 (2015).